



**X-1 Experiment Chamber Design and  
Analysis: 1998 Annual Report to Sandia  
National Laboratories**

**R.R. Peterson, G.L. Kulcinski, E.A. Mogahed, H.Y. Khater,  
M.E. Sawan, I.N. Sviatoslavsky, P. Cousseau,  
J.F. Santarius, K. Olson, T. Utschig, D.L. Henderson,  
M.L. Corradini, R.L. Engelstad, G.A. Moses**

**December 1998**

**UWFDM-1090**

***FUSION TECHNOLOGY INSTITUTE***

***UNIVERSITY OF WISCONSIN***

***MADISON WISCONSIN***

### **DISCLAIMER**

This report was prepared as an account of work sponsored by an agency of the United States Government. Neither the United States Government, nor any agency thereof, nor any of their employees, makes any warranty, express or implied, or assumes any legal liability or responsibility for the accuracy, completeness, or usefulness of any information, apparatus, product, or process disclosed, or represents that its use would not infringe privately owned rights. Reference herein to any specific commercial product, process, or service by trade name, trademark, manufacturer, or otherwise, does not necessarily constitute or imply its endorsement, recommendation, or favoring by the United States Government or any agency thereof. The views and opinions of authors expressed herein do not necessarily state or reflect those of the United States Government or any agency thereof.

**X-1 Experiment Chamber Design and Analysis:  
1998 Annual Report to Sandia National Laboratories**

R.R. Peterson, G.L. Kulcinski, E.A. Mogahed, H.Y. Khater, M.E. Sawan,  
I.N. Sviatoslavsky, P. Cousseau, J.F. Santarius, K. Olson, T. Utschig,  
D.L. Henderson, M.L. Corradini, R.L. Engelstad, G.A. Moses

Fusion Technology Institute  
Department of Engineering Physics  
University of Wisconsin-Madison  
1500 Engineering Drive  
Madison, WI 53706

December 1998

UWFDM-1090

1. Executive Summary .....	1
2. Experiment Chamber Design.....	4
2.1 Overall Strategy.....	4
2.2 Driver Interface.....	4
2.2.1 Long MITL Option.....	5
2.2.2 Water Transformer Option.....	6
2.3 MITL.....	6
2.4 Mini-Chamber.....	7
2.5 Cryogenic Systems.....	7
2.6 Chamber Wall and Liner.....	8
2.7 Shield.....	8
2.8 Diagnostics.....	9
2.9 Critical Issues .....	10
3. X-1 Target .....	10
3.1 Design.....	10
3.2 Emissions.....	11
3.2.1 X Rays .....	11
3.2.2 Debris .....	12
3.2.3 Neutrons .....	13
3.3 Development Needs.....	13
4. Blast Analysis.....	14
4.1 Analysis Methods.....	14
4.2 Mini-Chamber.....	15
4.3 Chamber Liner.....	18
4.4 MITL and Insulator Stack .....	20
4.5 Development Needs.....	22
5. Conclusions.....	23

Appendix

## 1. Executive Summary

The preliminary analysis of the X-1 experiment chamber has been conducted and several issues have been identified for further work. The X-1 experiment chamber will experience a considerably harsher environment than does the NIF chamber. Even in the case of no thermonuclear target yield, the energy in the X-1 chamber is conservatively estimated to be 20 MJ in magnetic debris and 16 MJ in x-rays. If a thermonuclear target yield of 200 MJ is achieved, another 60 MJ of target debris and x-rays and 140 MJ of neutrons are added. Without yield NIF will produce only approximately 1 MJ of x-rays, 0.8 MJ of debris, plus reflected or unabsorbed laser light. An ignited target NIF would add about 3 MJ in x-rays and 1 MJ of debris. Because the NIF target chamber was designed to be just below the vaporization threshold and is quite large (5.5 m radius), the much larger energies make it practically impossible to avoid substantial vaporization and melting in the X-1 experiment chamber. The fusion neutrons from yield shots and, to a lesser degree, photo-neutrons and ions will activate the experiment chamber. The challenge of the X-1 design activity is to develop an experiment chamber concept that allows radioactive vapor, molten material and shrapnel to be contained in a way that allows for timely maintenance and operation.

The experiment chamber concept is depicted in Figure 1.1. The design employs a “defense in depth” strategy. Multiple layers of protection are used to confine the blast generated by the energy contained in the chamber. The first level of protection is the hemispherical mini-chamber made of Kevlar with a graphite inner coating, which it meant to stop the large pieces of magnetic debris, and most of the x rays and debris ions emitted by the target. The mini-chamber may need replacement after shots with a burning ICF capsule, but it will be designed not to become a debris source itself. The next layer is an aluminum liner that will absorb those x-rays and debris ions that pass through holes in the mini-chamber. Both the liner and the mini-chamber will experience significant vaporization and melting. After a shot, the liner can be removed as a unit with the radioactive rubble trapped inside. Fast-closing explosive valves will prevent radioactive debris from leaving the experiment chamber. Outside, the liner is an aluminum structural wall designed to carry the impulsive and long-term pressure loading from the blast. Outside of that is a water shield to stop fusion neutrons and gamma rays emitted by radioactive materials.

This experiment chamber concept is flexible with respect to its pulsed power interface. There are at least two types of pulsed power options for X-1. One has many coaxial long magnetically insulated transmission lines (MITL's) that converge on the equatorial waist of the cylindrical experiment chamber. These MITL's can traverse space of almost any type: air, water, or solid shield. In this experiment chamber concept, the MITL's are surrounded by air for many meters, then by 2.5 m of water before joining the experiment chamber. Several MITL's are connected by a few conical MITL's inside the experiment chamber. Magnetic insulation is continuous across the experiment chamber wall. Therefore, no insulator stack is required.

In the other main type of pulsed power, a very thick water tank surrounds the chamber, which contains many water transformers. This concept also uses conical MITL's inside the chamber, but since the magnetic insulation begins at the chamber wall, an insulator stack is required. The only major difference between the experiment chambers for the two pulsed power concepts is the presence of a plastic insulator stack. The survival issues for this insulator stack are discussed herein. It is clear that a failure of the stack would allow the mixing of a large volume of tritiated water with the radioactive rubble inside the chamber and must be avoided at all cost.

The experiment chamber design must also be flexible in its use. At the recent workshop on Applications of Pulsed Power to Stockpile Stewardship in Las Vegas, Nevada, experiments to study radiation effects,

equation-of-state, opacity, fluid instabilities, mix, and radiation flow were suggested for X-1. These experiments could be performed for both ignited targets and no yield shots. The expected yield for these experiments could have a wider range than has yet been studied for the X-1 experiment chamber. Also, the relative energies in debris, x-rays and neutrons will vary among these experiment types. Diagnostic access will also vary. Radiation effects experiments will require large test samples with debris mitigation and large x-ray scattering structures. The design can be adapted to accommodate these experiments.

The University of Wisconsin has performed preliminary analysis of some aspects of this experiment chamber concept. These include the target-generated blast, the mechanical response of the experiment chamber to these blasts, and neutronics and radioactivity. The analysis assumes that the target x-ray, debris ion and neutron emissions have the same spectra as in the LIBRA-SP target, but that the energy release is scaled to 200 MJ of yield. Target emission calculations for an X-1 target concept are in progress, but are not yet used in the experiment chamber response analysis. The target x-rays and debris ions vaporize significant amounts of material from the mini-chamber, 0.247 kg for 200 MJ yield and 0.142 kg for the no thermonuclear yield case. The vaporization imparts a large recoil impulse to the chamber wall and mini-chamber, which might lead to mechanical failure. The mini-chamber receives impulses of 136 and 67 Pa-s with or without thermonuclear yield, while the chamber wall liner impulse is 41.2 or 18.4 Pa-s. Mechanical analysis has been performed for the wall liner, but not the mini-chamber. There is confidence that vessels can be designed to withstand such impulses. The biological dose rate has been calculated for 200 MJ yield shots, and it has been found that the chamber concept allows access to the back of the water shield a few hours after a shot and hands-on access to the chamber wall 10 days after the shot. For no thermonuclear yield, access is allowed through the experiment chamber several hours after a shot.

A number of critical issues remain for the X-1 experimental chamber. They should be addressed during the conceptual design of X-1 as well as throughout the construction and operation of X-1. These include the following:

- Remote maintenance and removal of an experimental chamber after a yield shot and minimization of facility downtime.
- X-ray, debris, and neutron output from all likely experiments.
- Production of secondary debris by interaction of the target emissions with the target support structures and power feeds.
- Exact determination of impurities present and chamber materials, including structures and diagnostics and calculation of radioactivity and biological dose rates due to these impurities.
- Fragmentation of mini-chamber, cryogenic equipment, and diagnostics into damaging shrapnel and the effects that shrapnel might have on the experimental chamber.
- Migration of radioactive rubble into diagnostic and pulsed power ports and the design of fast-closing valves.
- Effect of diagnostics and pulsed power ports and conical MITL's on the dynamics of experimental chamber.
- Verification of all computer codes used in the experiment chamber design through experiments.

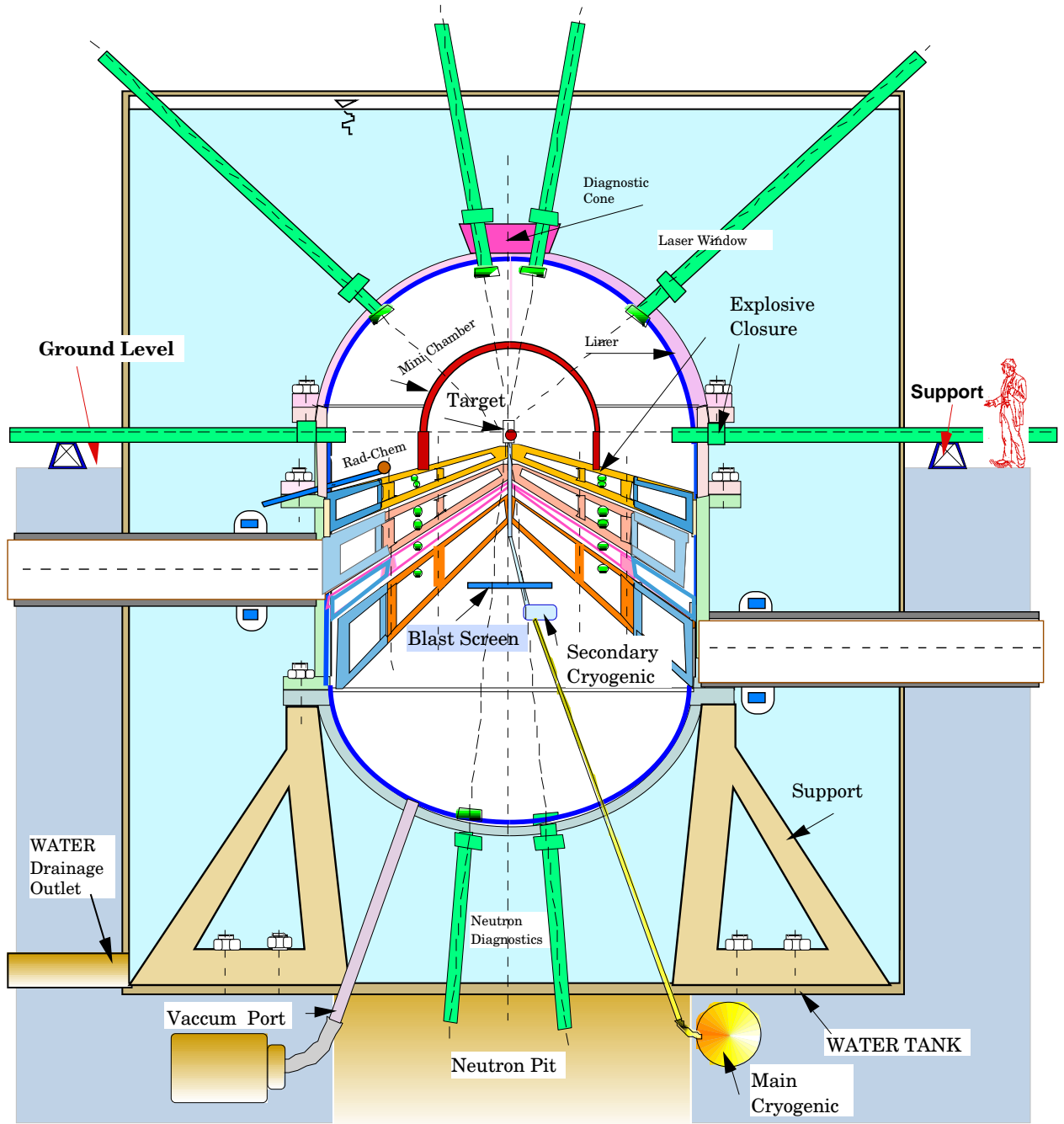


Figure 1.1. X-1 experiment chamber design concept. The chamber is shown for the long MITL option and for a target driven by one-sided power feeds.

## 2. Experiment Chamber Design

### 2.1 Overall Strategy

The experiment chamber concept is depicted in Figure 1.1. The design employs a “defense in depth” strategy. Multiple layers of protection are used to confine the blast generated by the energy contained in the chamber. The first level of protection is the hemispherical mini-chamber made of Kevlar with a graphite inner coating, which it meant to stop the large pieces of magnetic debris, and most of the x rays and debris ions emitted by the target. The mini-chamber may need replacement after shots with yield, but it will be designed not to become a debris source itself. The next layer is an aluminum liner that will absorb those x-rays and debris ions that pass through holes in the mini-chamber. Both the liner and the mini-chamber will experience significant vaporization and melting. After a shot, the liner can be removed as a unit with the radioactive rubble trapped inside. Fast-closing explosive valves will prevent radioactive debris from leaving the experiment chamber. In back of the liner is an aluminum structural wall to carry the impulsive and long-term pressure loading from the blast. Outside of that is a water shield to stop fusion neutrons and gamma rays emitted by radioactive materials.

The X-1 experiment chamber will experience a considerably harsher environment than does the NIF experiment chamber. Even in the case of no thermonuclear target yield, the energy in the X-1 chamber is conservatively estimated to be 20 MJ in magnetic debris and 16 MJ in x-rays. If 200 MJ of thermonuclear target yield are present, another 60 MJ of target debris and x-rays and 140 MJ of neutrons are added. Without yield NIF will produce approximately 1 MJ of x rays and 0.8 MJ of debris and reflected or unabsorbed laser light, to which an ignited target would add about 3 MJ in x-rays and 1 MJ of debris. Because the NIF experiment chamber was designed to be just below the vaporization threshold and is quite large (5.5 m radius), the much larger energies make it practically impossible to avoid substantial vaporization and melting in the X-1 experiment chamber. The fusion neutrons from yield shots and, to a lesser degree, photo-neutrons and ions will activate the experiment chamber. The challenge of the X-1 design activity is to develop an experiment chamber concept that allows radioactive vapor, molten material and shrapnel to be contained in a way that allows for timely maintenance and operation.

The experiment chamber design must also be flexible in its use. At the recent Workshop on Applications of Pulsed Power to Stockpile Stewardship, experiments to study radiation effects, equation-of-state, opacity, fluid instabilities, mix, and radiation flow were suggested for X-1. These experiments could be performed for both ignited targets and no yield shots. The expected yield for these experiments could have a wider range than has yet been studied for the X-1 experiment chamber. Also, the relative energies in debris, x-rays and neutrons will vary among these experiment types. Diagnostic access will also vary. Radiation effects experiments will require large test samples with debris mitigation and large x-ray scattering structures. The design can be adapted to accommodate these experiments.

### 2.2 Driver Interface

This experiment chamber concept is flexible in its pulsed power interface. There are at least two types of pulsed power options for X-1. One has many coaxial long magnetically insulated transmission lines (MITL's) that converge on the equatorial waist of the cylindrical experiment chamber. These MITL's can traverse space of almost any type: air, water, or solid shield. In this experiment chamber concept, the MITL's go through air for many meters and then through 2.5 m of water before joining the

experiment chamber. The many long MITL's connect to a few conical MITL's inside the experiment chamber, shown in Figure 2.2.1. Magnetic insulation is continuous across the experiment chamber wall. Therefore, no insulator stack is required. In the other main type of pulsed power, a very thick water tank surrounds the chamber, which contains many water transformers. This concept also uses conical MITL's inside the chamber, but since the magnetic insulation begins at the chamber wall, an insulator stack is required. So, the only major difference between the experiment chambers for the two pulsed power concepts is the presence of a plastic insulator stack. The survival issues for this insulator stack are discussed herein, where it is clear that a failure of the stack would allow the mixing of a large volume of tritiated water with the radioactive rubble inside the chamber and must be avoided at all cost.

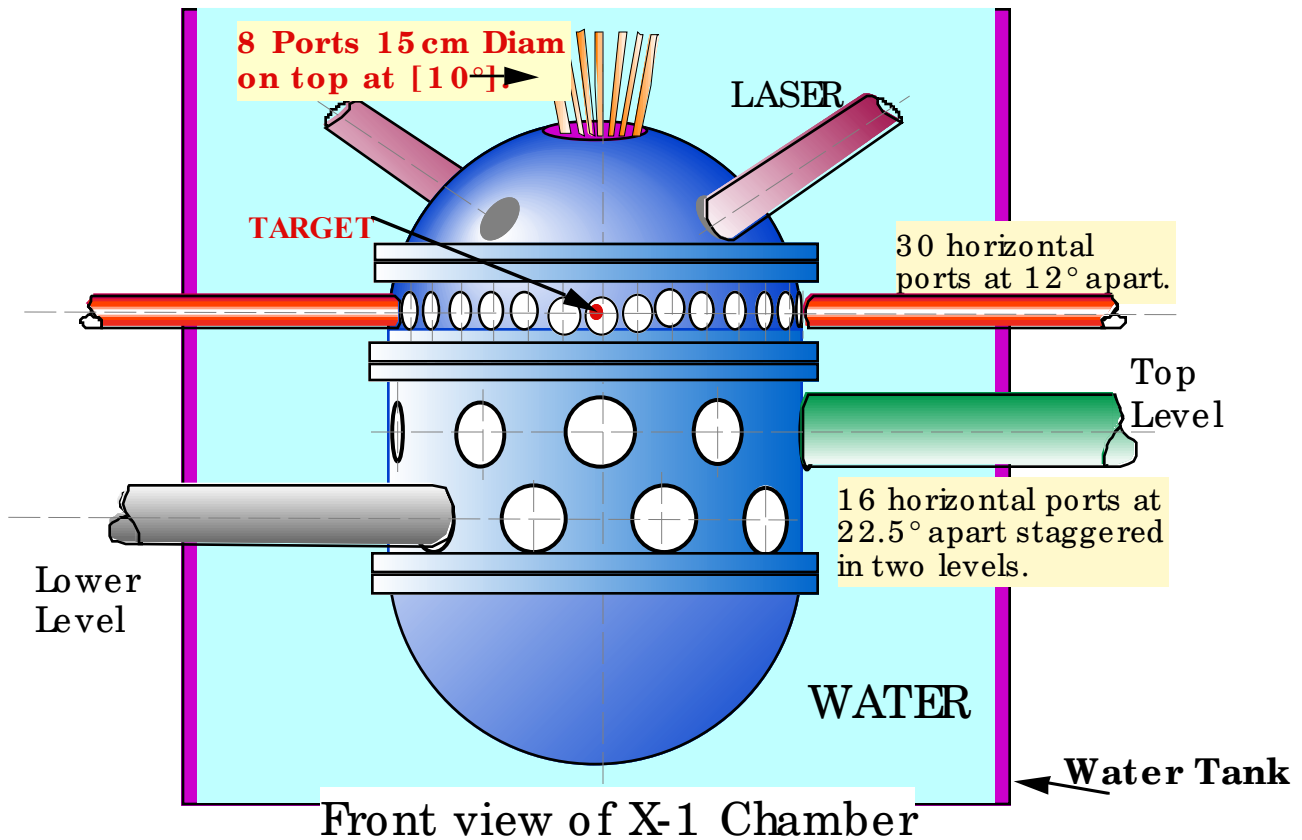


Figure 2.2.1. External view of X-1 experiment chamber design concept. The chamber is shown for the long MITL option.

### 2.2.1 Long MITL Option

In the long MITL option, there are approximately 40 coaxial transmission lines that intersect the experimental chamber wall in two rows of 20. This is schematically shown in Figure 2.2.1. Each of the lines is about 70 cm in diameter. The transmission lines begin to touch each other at a radius of 225 cm from the target. The experiment chamber wall is 250 cm from the target, so there is some space between the transmission lines at the chamber boundary. At this point the transmission lines make a transition to a few disk conductors. These are separated by gaps of a few cm and carry the current to the region of the target. The transition to disks occurs over a distance of about a meter, as shown in Figure 2.3.1. In this

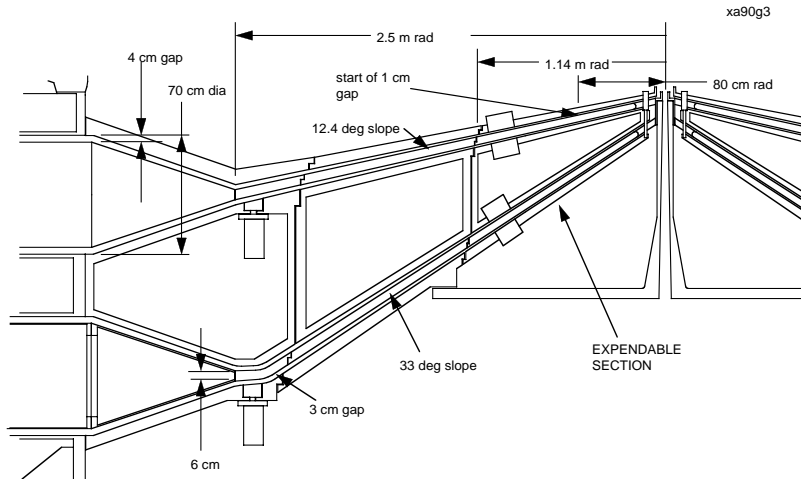
pulsed power scheme, the same vacuum system extends over many tens of meters from the inductive driver modules to the target. The inner conductors are either cantilevered from the back of the driver module or are temporarily supported closer to the chamber. In the chamber concept, the transmission lines are inside a water tank from the last 250 centimeters before the chamber wall. The region inside the inner conductor of the coaxial lines may be filled with some neutron shielding material.

### 2.2.2 Water Transformer Option

In the water transformer option, the driver consists of a large number of Marx generators in a large oil-filled tank, which in turn drive large parallel plate transmission lines in water. Here the system is arranged like the Z machine, with an outer annular oil tank around an inner annular water tank. The parallel plate lines may initially be tall vertical plates that feed into several large horizontal disk plates. These connect to plastic insulators at the experiment chamber wall. Here the water serves a dual purpose; it is the dielectric medium for the transmission lines and it is a neutron shield. The vacuum boundary is at the insulator stack. The vacuum region in this option is similar to the chamber region of the long MITL concept, with several conical disk MITL's.

### 2.3 MITL

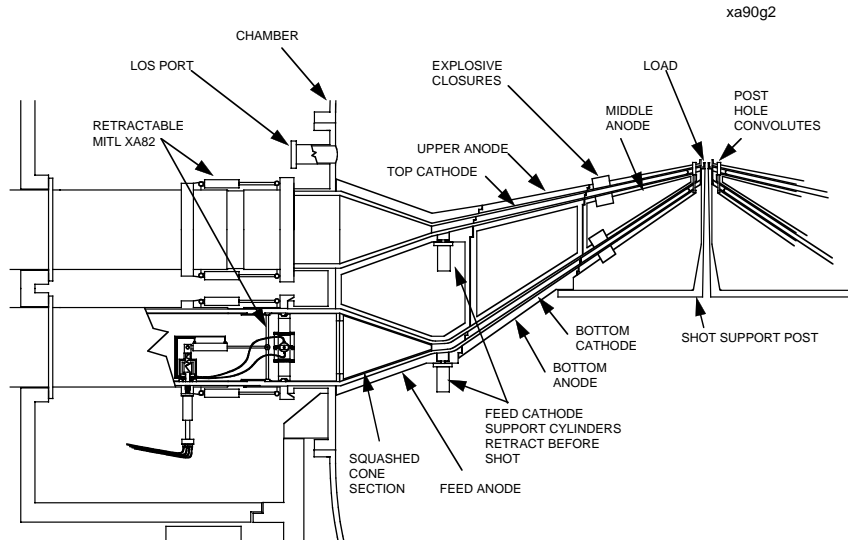
The conical MITL's in the target chamber are similar for both driver options. A design for the long MITL option is shown in Figures 2.3.1 and 2.3.2. Here, one sees five conical conductors linked to two layers of co-axial transmission lines. The gap between conductors is 3 cm near the chamber wall, but it reduces to 1 cm near the target. The MITL's consist of three sections: within 1.14 meters of the target, between 1.14 m and about 2 m, and from 2 m from the target to the co-axial transmission lines. The inner two sections are constructed of steel; the outer section is aluminum. One can see in Figure 2.3.2 that the inner conductor of the co-axial MITL's has retractable support cylinders. This must be rapidly removed shortly before each shot.



Xa90 Chamber Concept Date 5-12-98

SHEET 3

Figure 2.3.1. Conical MITL's in X-1 experimental section. Details of in-chamber components.



Xa90 Chamber Concept Date 5-12-98

SHEET 2

Figure 2.3.2. Conical MITL's in X-1 experimental section. Details of transition for co-axial to conical transmission lines are shown, including temporary supports.

## 2.4 Mini-Chamber

A mini-chamber is used in X-1 to prevent energetic shrapnel from damaging the experiment chamber. The mini-chamber is a hemispherical shell 1 m in radius centered on the target. The mini-chamber is constructed of Kevlar with an inner liner of graphite. The Kevlar stops the energetic shrapnel without becoming shrapnel itself. The graphite absorbs the target x-rays and debris and minimizes the vaporization and recoil impulse of the mini-chamber. The mini-chamber has holes for diagnostics and for radiation effects experiments, but most of the vapor, debris and shrapnel remain trapped inside the mini-chamber. It is expected that the mini-chamber will survive several radiation shots with no thermonuclear yield, but that shots with yield may damage the mini-chamber enough that it would be replaced.

Vaporized remnants of the target will adhere to the mini-chamber. Fusion and photo-neutrons will activate this target debris, which can become a major source of radioactivity if the material remains in the experiment for many yield shots. However, the mini-chamber will likely be removed after high yield shots so the radioactivity in the target debris may become a manageable part of the waste stream.

## 2.5 Cryogenic Systems

Some of the target capsules used in X-1 will be cryogenic. These are spherical hollow shells made of either Be or plastic that are pressurized with DT. These targets have to be maintained cold while in the chamber prior to being imploded. For this reason some form of cryogenic system is needed. Spherical shells made from Be are strong and can be filled with DT gas prior to freezing. Such targets can be placed in the hohlraum at the center of the chamber manually during assembly of the MITL's. A cryogenic system is then needed to liquefy and freeze the DT in situ. Plastic targets are not strong enough to withstand the

DT gas pressure and therefore have to be cooled outside the chamber, then inserted into the chamber and maintained cold before they are imploded. For this, a remote manipulator is needed to insert the target into the wire array and the hohlraum at the center of the chamber.

Two cryogenic systems are being considered for the X-1 chamber. One system has a small low cost cryogenerator attached to the bottom of the chamber with only electrical leads penetrating the chamber through a bottom feedthrough. The other system has a cryogenerator located outside the chamber, but has He gas lines penetrating the chamber through a feedthrough. The cold He gas keeps the target cold until the time of the shot, when the He lines are valved off. Trade studies will be performed to evaluate the two systems with respect to practicality and cost before adopting the baseline design.

## 2.6 Chamber Wall and Liner

The X-1 experiment chamber wall and liner are designed to contain the blast generated by the target x-rays and debris. The liner is an aluminum shell that rests on and is supported by an aluminum structural wall. The mini-chamber prevents damage to the liner by shrapnel, but some target x rays and ion debris will reach the liner by passing through holes in the mini-chamber. These will vaporize material in localized spots on the liner which will lead to recoil pressure in those regions. Shocks generated in the liner will dissipate before reaching the structural wall. The wall and liner will have diagnostics and pulsed power holes. These holes will be behind debris mitigation systems that prevent radioactive material from passing out of the experiment chamber.

Radioactive rubble will be contained inside the liner. The debris mitigation systems at the port will consist of baffles and fast closing explosive valves. After a high yield shot the large amount of radioactive rubble from the MITL's and target will remain trapped in the liner. The whole inside of the experiment chamber can be remotely removed inside the liner and disposed of. The liner would then be replaced and new MITL's added. This will significantly reduce the time between shots because much of the radioactive material would be removed. The structural wall would become the major source of radioactivity that remains in the facility from shot to shot and whose cool-down time has an impact on operations.

## 2.7 Shield

The experiment chamber is surrounded by a 2.5-m thick water shield. This shield results in attenuating the neutron flux and reducing the activation of equipment and material present inside the experiment chamber building. In particular, diagnostics equipment will be placed in back of the shield and may contain materials susceptible to neutron activation. The size of the water shield was determined to allow quick access to the inside of the building following shots. The radial variation of the neutron and gamma fluences in the part of the experiment chamber above ground is shown in Figure 2.7.1. The results are given for the 200 MJ yield shots. Secondary gamma photons are produced by neutron interactions in the chamber wall and liner. While 27 cm of water shielding attenuates the neutron fluence by an order of magnitude, 60 cm is required for an order of magnitude attenuation in gamma fluence. The peak leakage fluences at the top surface of the water shield tank are  $1.6 \times 10^4$  n/cm<sup>2</sup> and  $4.9 \times 10^9$  γ/cm<sup>2</sup>. The peak leakage fluences at the side of the tank just above ground are  $8.0 \times 10^3$  n/cm<sup>2</sup> and  $2.2 \times 10^9$  γ/cm<sup>2</sup>. The total numbers of neutrons and gamma photons leaking from the shield tank are  $3.1 \times 10^9$  neutrons and  $1.6 \times 10^{15}$  gamma photons, respectively, for a 200 MJ shot. Although the amount of leaking gamma photons is relatively large, this is not of concern since they will not activate the material outside the shield tank.

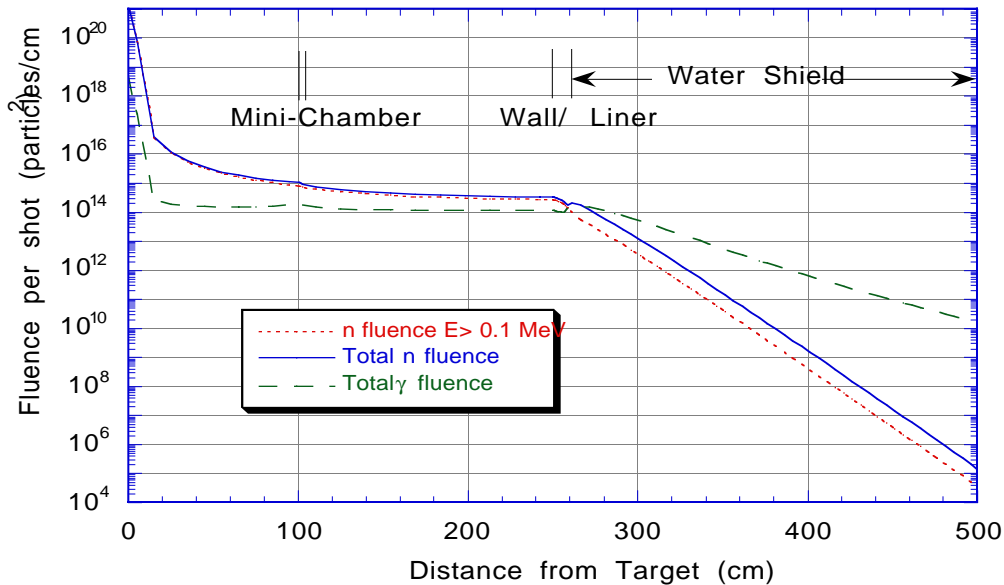


Figure 2.7.1. Neutron and gamma fluence variation in the X-1 chamber for a 200 MJ shot.

## 2.8 Diagnostics

The purpose of X-1 is to perform experiments related to high energy density physics, many of which need to be defined. Adequate diagnostics are required for these experiments to be successful. The diagnostic needs of X-1 will evolve as experiments are defined throughout the lifetime of the facility. Therefore, the X-1 concept should be able to accommodate as wide a variety of diagnostics as possible. To insure the best possible integration of diagnostics into the X-1 experiment chamber concept, a list of likely diagnostics has been completed for X-1. This list is included in the appendix. This list includes all of the NIF diagnostics<sup>1</sup> except those specific to the driver laser. To this, additional diagnostics have been included for pulsed power.

The diagnostics include instruments to measure temporally, spectrally and spatially resolved photons, ions and neutrons. The diagnostics must be placed in positions dictated by the experiments. Many of the experiments will require horizontal diagnostic access. Some neutron diagnostics need long lines of sight (LOS), which can only be done horizontally. Some neutron diagnostics will be placed in a neutron pit below the target chamber. Some photon diagnostics need vertical access. Finally, two backlighter lasers are required that have been placed at 45° above the horizontal plane, though it may be possible to place them horizontally.

Many of the instruments will be placed in or in back of the biological shield. The ports and diagnostic tubes will have an impact on the behavior of the target chamber. To mitigate pipe-shine, diagnostic design favors large aperture ports and tubes. Large aperture ports lead to stress concentrations in the chamber wall that must be accommodated in the chamber design. Also, ports allow the leakage of neutrons through the chamber wall and shield that cause activation. Shielding must be designed to control biological dose rates in these regions.

## 2.9 Critical Issues

A number of critical issues remain for the X-1 experimental chamber. They should be addressed in the concept design of X-1 and throughout the building and operation of X-1. These include the following:

- Remote maintenance and removal of an experimental chamber after a yield shot and minimization of facility downtime.
- X-ray, debris, and neutron output from all likely experiments.
- Production of secondary debris by interaction of the target emissions with the target support structures and power feeds.
- Exact determination of impurities present and chamber materials, including structures and diagnostics and calculation of radioactivity and biological dose rates due to these impurities.
- Fragmentation of mini-chamber, cryogenic equipment, and diagnostics into damaging shrapnel and the effects of that shrapnel on the experimental chamber.
- Migration of radioactive rubble into diagnostic and pulsed power ports and the design of fast-closing valves.
- Effect of diagnostics and pulsed power ports and conical MITL's on the dynamics of the experimental chamber.
- Verification of all computer codes used in the experiment chamber design through experiments.

### Reference for Section 2.8

1. R.J. Leeper, et al., "Target Diagnostics for the National Ignition Facility", *Rev. Sci. Instrum.*, 68, 868 (January 1997).

## 3. X-1 Target

At least three target concepts are under consideration for yield targets on X-1. Here, one concept is used to provide a context in which to discuss issues of target cryogenics and coupling to the pulsed power. To provide target emissions needed to analyze the X-1 experiment chamber, typical ICF target spectra have been chosen.

### 3.1 Design

An X-1 target might look like the target depicted in Figure 3.1.1. This is a Sandia National Laboratories concept, where x-rays drive a cryogenic fusion capsule to implosion from two z-pinchs positioned at either ends of a cylindrical hohlraum. The concept in Figure 3.1.1 feeds electrical power to both z-pinchs from the same side. This will make experiment design and diagnostics much more flexible, but this concept has a higher inductance than driving the z-pinchs from two sides. Therefore, pulsed power voltage or rise time must be balanced against flexibility of X-1 experiments. A cryogenic helium feed tube is shown in the figure. Open-cell plastic foam fills the region inside the hohlraum and around the fuel capsule. Helium flows through the foam, cooling the capsule.

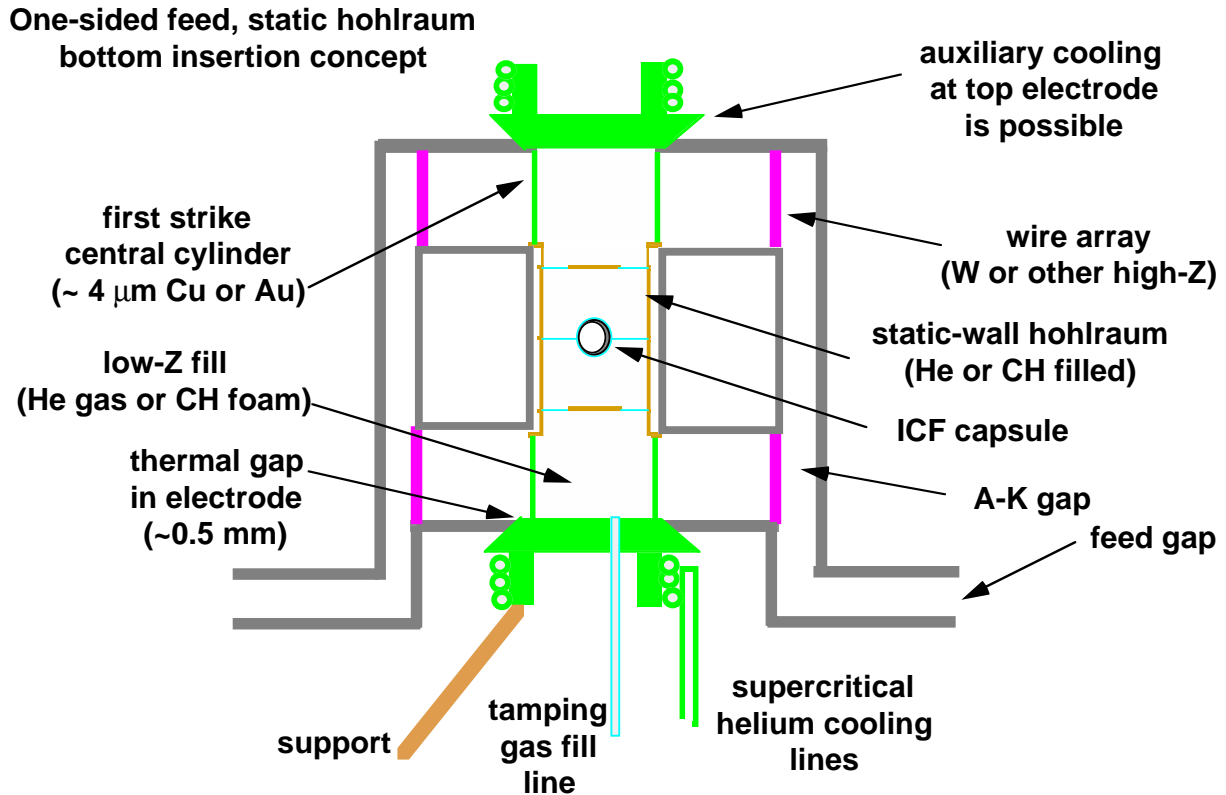


Figure 3.1.1. Sandia National Laboratories X-1 target concept. Pulsed power feeds from one side.

### 3.2 Emissions

Work is in progress on the calculation of x-ray, ion and debris emission from the X-1 target shown in Figure 3.1.1. This is being done with the BUCKY computer code<sup>1</sup>. Until those simulations are complete, we are using target x-ray and ion debris spectra from the LIBRA-SP<sup>2</sup> study and NIF.

#### 3.2.1 X Rays

The X-1 target will emit substantial energy in x-rays. X rays are produced in a burning ICF target or by a z-pinch. In the X-1 target, the capsule expands at great speed ( $\cong 10^8$  cm/s), but because it is fully ionized x-ray emission is in Bremsstrahlung and only moderate. When the capsule collides with the gold hohlraum case and stagnates, the kinetic energy of the capsule is converted into internal energy of the gold/capsule mixture. This stagnated plasma radiates x-ray energy. Therefore, the x-ray emission power is the double pulse shown in Figure 3.2.1.1. The X-1 target x-ray spectrum will be mostly due to emission from the stagnated gold/capsule plasma. This emission is typically a blackbody spectrum at about 400 eV. There is some x-ray emission from the capsule that penetrates the gold hohlraum. The capsule is burning at a temperature of several tens of keV and gold has a reduced opacity around 50 keV. The spectra emitted by the LIBRA-SP target<sup>3</sup>, integrated up to various times are shown in Figure 3.2.1.2.

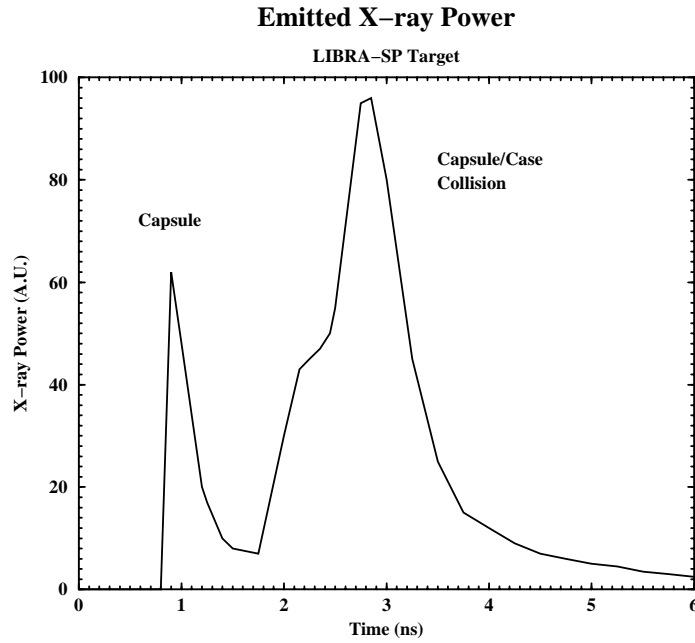


Figure 3.2.1.1. X-ray emission power from LIBRA-SP target.

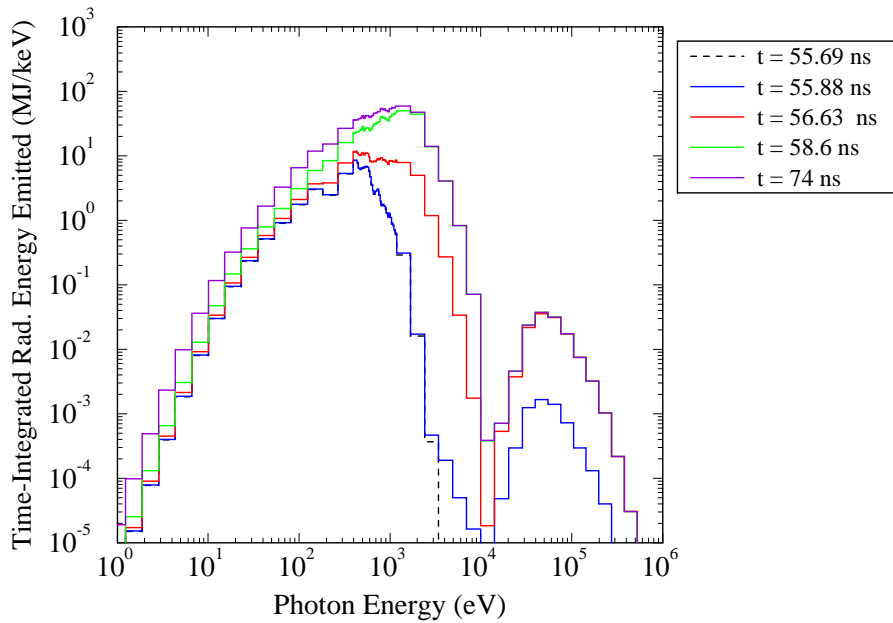


Figure 3.2.1.2. X-ray emission spectrum from LIBRA-SP target.

### 3.2.2 Debris

The ion debris from the X-1 target contains whatever energy deposited in or generated by the target that has not been radiated away as neutrons or photons. The energy density is such that the hohlraum and capsule are assumed to be totally vaporized. As the vapor expands, the internal energy is converted into directed kinetic energy. The density of the vapor continually drops until the atomic collisions become so infrequent that the vapor is no longer properly thought of as a fluid, but is just a collection of ions and

electrons moving in straight lines. We assume that the electrons and ions are moving together so there is charge neutrality in the vapor. Because the internal energy of the vapor becomes low, there is a possibility that the vapor could re-condense into droplets. However, the density of the vapor at this point is low enough that the re-condensation time should be much longer than the time of flight of the ions to the first surface. Calculations of debris ion spectra have been done with the BUCKY code for several target designs, but have not been done yet for X-1. In these calculations, the velocities and densities of all Lagrangian zones are recorded at the end of a long simulation of the breakup of a target and an ion energy spectrum is determined. Based on our experience with the NIF target<sup>4</sup>, we expect X-1 to have ion velocities on the order of  $10^7$  cm/s or gold ion energies of 10 keV.

### 3.2.3 Neutrons

Due to (n, 2n) and (n, 3n) reactions occurring in the target, 1.042 neutrons are emitted from the target for each DT fusion reaction. These neutrons carry a total energy of 12.29 MeV implying that the average energy of neutrons emitted from the target is 11.8 MeV. For each DT fusion reaction, 0.0033 gamma photons are emitted from the target with an average energy of 3.66 MeV. For a 200 MJ shot, the total numbers of neutrons and gamma photons emitted from the target are  $7.4 \times 10^{19}$  neutrons and  $2.3 \times 10^{17}$  gamma photons, respectively. The energy spectrum of neutrons emitted from the target is shown in Figure 3.2.3.1.

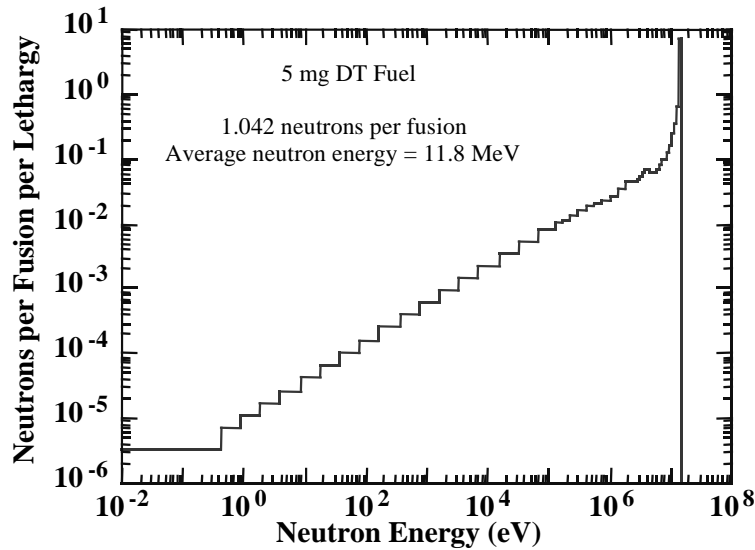


Figure 3.2.3.1. Energy spectrum of neutrons emitted from the target.

### 3.3 Development Needs

Since the target emissions drive the chamber design they need to be better understood. Analysis and validation of analysis methods both need more work.

- Complete 1-D BUCKY analysis of baseline X-1 high yield target concept. This will provide reasonable x-ray, neutron, and ion emission spectra for experiment chamber considerations.
- Perform 1-D BUCKY simulations of the x-ray emission spectra from z-pinch targets with no fusion yield.

- Perform 1-D BUCKY simulations of high energy density experiments that might be fielded in X-1 to provide x-ray and debris source terms for chamber analysis.
- Perform 2 or 3-D analysis of the radiative breakup of baseline X-1 target, to get angle-dependent emission.
- Using 1, 2, and 3-D analysis calculate the generation of secondary debris emission from target support structures such as current return cans, diagnostics, and cryogenic system.
- Devise and perform experiments to validate the emission predictions by BUCKY and other codes. These would include z-pinch experiments on Z or Saturn, colliding-plasma experiments on Omega or Trident, and debris emission experiments.

#### References for Sections 3.2 - 3.2.2

1. MacFarlane, J.J., G.A. Moses, and R.R. Peterson, "BUCKY-1 - A 1-D Radiation Hydrodynamics Code for Simulating Inertial Confinement Fusion High Energy Density Plasmas", University of Wisconsin Fusion Technology Institute Report UWFD-984 (August 1995).
2. Badger et al., "LIBRA-SP -- A Light Ion Fusion Power Reactor Design Study Utilizing a Self-Pinched Mode of Ion Propagation", University of Wisconsin Fusion Technology Institute Report UWFD-983 (June 1995).
3. MacFarlane, J.J., M.E. Sawan, G.A. Moses, P. Wang, and R.E. Olson, "Numerical Simulations of the Explosion Dynamics and Energy Release from High-Gain ICF Targets", University of Wisconsin Fusion Technology Institute Report UWFD-1026 (June 1996).
4. Peterson, R.R. et al., "Target Emission and Wall Response: National Ignition Facility Target Area Studies Interim Report for the Period 5/1/95 through 3/31/96", University of Wisconsin Fusion Technology Institute Report UWFD-1008 (April 1996).

## 4. Blast Analysis

The University of Wisconsin has performed preliminary analysis of some aspects of this experiment chamber concept. These include the target-generated blast and the mechanical response of the experiment chamber to these blasts. The analysis assumes that the target x-ray, debris ion and neutron emissions have the same spectra as in the LIBRA-SP target<sup>1</sup>, but that the energy release is scaled to 200 MJ of yield. Target emission calculations for an X-1 target concept are in progress, but are not yet used in the experiment chamber response analysis. The target x-rays and debris ions vaporize significant amounts of material from the mini-chamber, 0.247 kg for 200 MJ yield and 0.142 kg for no thermonuclear yield. The vaporization imparts a large recoil impulse to the chamber wall and mini-chamber, which might lead to mechanical failure. The mini-chamber receives impulses of 136 and 67 Pa-s with or without thermonuclear yield, while the chamber wall liner impulse is 41.2 or 18.4 Pa-s. Detailed mechanical analysis has yet to be performed for the wall liner and mini-chamber, but vessels can be designed to withstand such impulses.

### 4.1 Analysis Methods

In the analysis of the blast response of the X-1 experimental chamber, the BUCKY computer code<sup>2</sup> has been used with equation-of-state and opacity data from SESAME<sup>3</sup> tables and EOSOPA<sup>4</sup> calculations. BUCKY is a 1-D Lagrangian radiation-hydrodynamics code in slab, cylindrical, and spherical geometry. BUCKY models MHD effects and accepts thermal photon, laser, non-thermal x-ray, and ion external

energy sources. BUCKY models thermonuclear burn with fusion product transport and is being used to study X-1 target implosions and burn. BUCKY can model phase changes in spherical, slab, and cylindrical solid or liquid regions adjacent to a plasma region. Energy is deposited on the surface of the solid or liquid region due to thermal conduction or thermal radiation from the plasma. X-ray and ion energy is deposited in the condensed matter volumetrically based on range-energy data. Thermal conduction in the liquid or vapor is calculated with temperature dependent thermal conductivities and heat capacities. Hydrodynamics is not modeled in solid or liquid regions, but when that material becomes vapor it joins the plasma region and the vapor moves into the plasma. If the condensed matter is modeled as part of a plasma region (SESAME and EOSOPA equations-of-state can model dense cold material), hydrodynamics can be calculated in solids or liquids, though the calculation of thermal conduction is not as accurate with this approach. BUCKY provides the time-dependent pressure and mass ablation rate on the surface of a material. The time-integrals of these give the impulse and total mass loss of the material. Also, the energy remaining in the vapor after the vapor stops radiating leads to a quasi-steady-state pressure. This residual pressure leads to an applied long-term load to the chamber that affects mechanical response. Assuming the vapor is  $\delta$ -law gas, the residual pressure is  $\delta$  times the vapor energy per unit volume.

## 4.2 Mini-Chamber

Using the analysis method described above, the responses of the X-1 mini-chamber to the explosion of a 200 MJ target and 16 MJ of z-pinch x-rays have been calculated in spherical geometry. The results are summarized in Table 4.2.1 for the vaporization of graphite. The target and pinch x-ray photons vaporize graphite from the inside of the mini-chamber. The mass vaporized from the mini-chamber for a 200 MJ target explosion is shown as a function of time in Figure 4.2.1, along with the x-ray power history. The effects of the target ion debris are not included in the vaporization because they arrive at the mini-chamber later in time than the x-ray photons and they are absorbed in the blow-off vapor. Their energy contributes to the residual pressure but not to the vaporization of recoil impulse on the structure. Figure 4.2.1 clearly shows that the vaporization follows the shape of the x-ray power curve. The residual pressure is 4.3 MPa, a substantial value. The vaporization leads to a recoil impulse of 136 Pa-s, which leads to significant vibrations in the mini-chamber. The peak pressure of 4.3 Mbar will clearly launch shocks into the graphite and Kevlar.

The effects of magnetic debris are not yet analyzed. Magnetic debris energy fluences are of the same magnitude as x rays and ion debris. The Kevlar in the main body of the mini-chamber is designed to absorb the energy of the magnetically accelerated projectiles without fracturing, though analysis of this phenomenon is needed. The projectiles will lead to cratering in the graphite and Kevlar.

The details of the vaporization process are depicted in Figure 4.2.2, where the mass density profiles of the vapor are shown. The vaporization occurs over about 5 ns, too short a time for the vapor to move very far. So the vapor remains near solid for several ns. The figure shows that the vapor at 20 ns after the start of the x-ray pulse is still to a large degree within 100  $\mu\text{m}$  of the surface and the density on the surface is still about a tenth of solid density. Since a 200 MJ target explosion vaporizes about 10  $\mu\text{m}$ , this density is consistent with the vapor motion. The pressure of a vapor at solid density and a few eV is in the Mbar range, so the instantaneous pressure is very high. The pressure on the surface is shown in Figure 4.2.3. This figure also shows the re-radiation of energy from the vapor to the surface, which is only 0.012 J/cm<sup>2</sup> so re-radiation is not important to the vaporization. Integrating the pressure over several ns leads to a large recoil impulse on the surface of the structure, which is also equal to the product of the average velocity and the mass of the vapor.

The response of the mini-chamber of a non-yield shot with 16 MJ of z-pinch x-rays is similar to the response to a 200 MJ shot, with somewhat less vaporization. The same x-ray spectrum has been assumed and is scaled to 16 MJ. A parametric study of response versus yield has been performed and the results are shown in Figure 4.2.4. Once again the x-ray spectrum and pulse shape discussed in section 3 are used and the photon fluence is scaled. It is seen that the response (peak pressure, impulse and mass vaporized) is close to linear in yield.

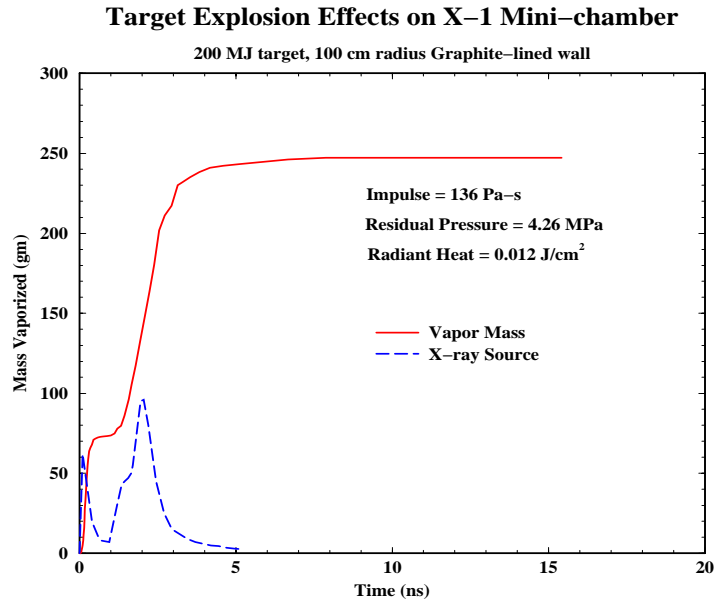


Figure 4.2.1. Mass vaporized from X-1 mini-chamber by x-rays from 200 MJ target explosion.

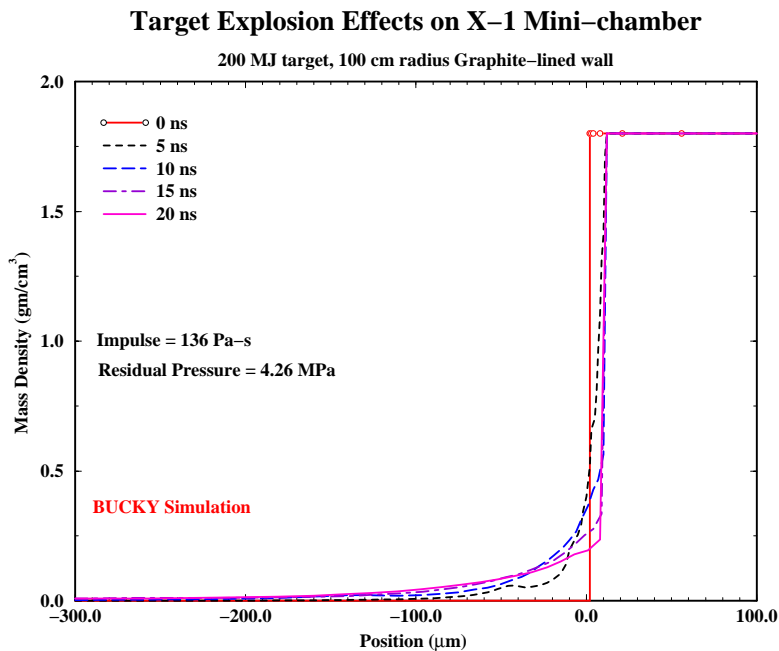


Figure 4.2.2. Mass density profiles on surface of X-1 mini-chamber due to x-rays from 200 MJ target explosion.

### Target Explosion Effects on X-1 Mini-chamber

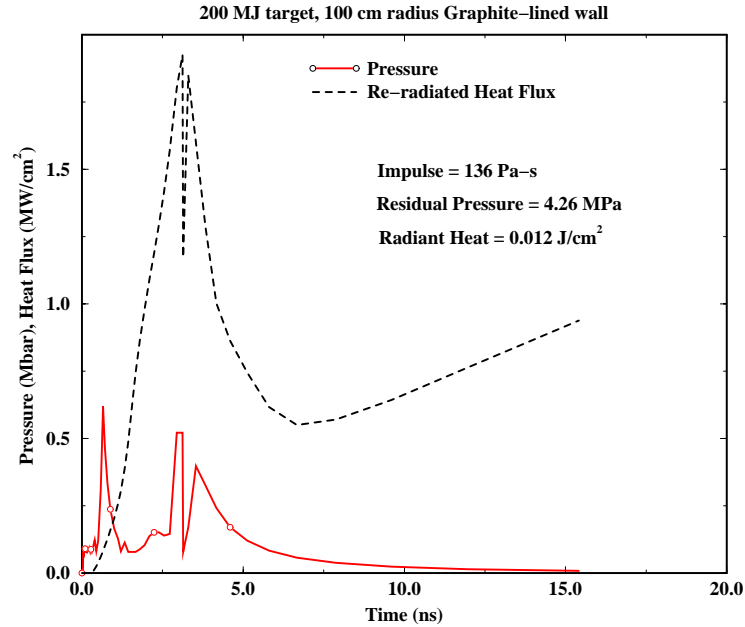


Figure 4.2.3. Pressure and heat flux on inner surface of X-1 mini-chamber due to x-rays from 200 MJ target explosion.

### Carbon X-1 Mini-Chamber

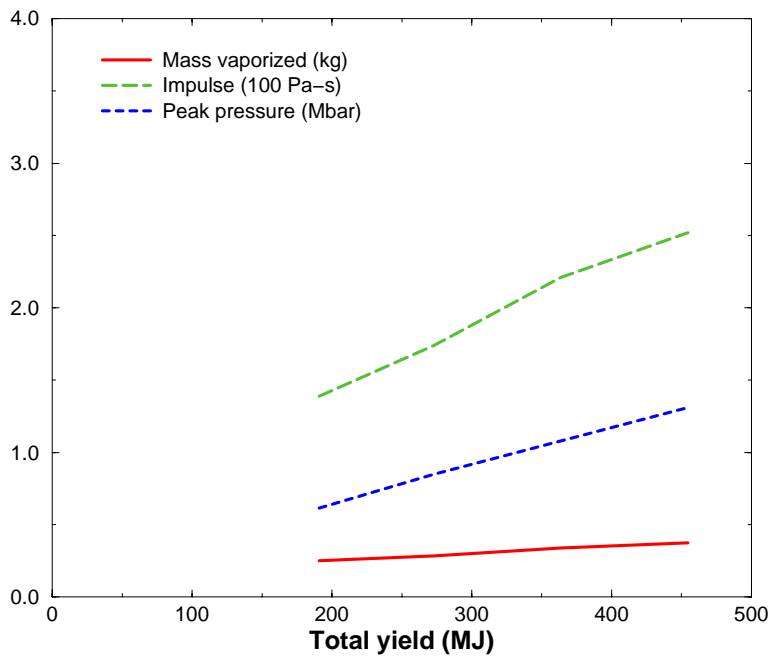


Figure 4.2.4. Mass vaporized, impulse and peak pressure on surface of X-1 mini-chamber as a function of target yield.

Table 4.2.1. Response of X-1 Mini-Chamber to Target Explosion

Fusion Yield (MJ)	0	200
X-ray Energy (MJ)	16	44
X-ray Fluence (J/cm <sup>2</sup> )	127	350
Debris Ion Energy (MJ)	0	12
Debris Ion Fluence (J/cm <sup>2</sup> )	0	95
Magnetic Debris Energy (MJ)	20	20
Magnetic Debris Fluence (J/cm <sup>2</sup> )	159	159
Vapor Mass (kg)	0.142	0.247
Impulse (Pa-s)	67	136
Peak Pressure (MPa)	$2.3 \times 10^5$	$6.2 \times 10^5$
Residual Pressure (MPa)	2.0	4.3

### 4.3 Chamber Liner

The response of the chamber liner is calculated in the same way as the mini-chamber. The mini-chamber has been removed in these calculations. There will be holes in the mini-chamber that allow x-rays and debris to reach the liner. These calculations put an upper limit on the damage caused by these target emissions because all x-rays and ions are assumed to leak through the mini-chamber. The results are summarized in Table 4.3.1, where results for no yield and 200 MJ and 1000 MJ are shown. The results for 200 MJ target yield are shown in Figures 4.3.1 and 4.3.2, where the vaporization of aluminum by target x-rays is shown. The results are qualitatively similar to the mini-chamber results. Like in the mini-chamber, debris ions only contribute to the residual pressure. Also, magnetic debris has yet to be considered. The results of a parametric study are shown in Figure 4.3.3. Just as in the mini-chamber, the response is close to linear in target yield.

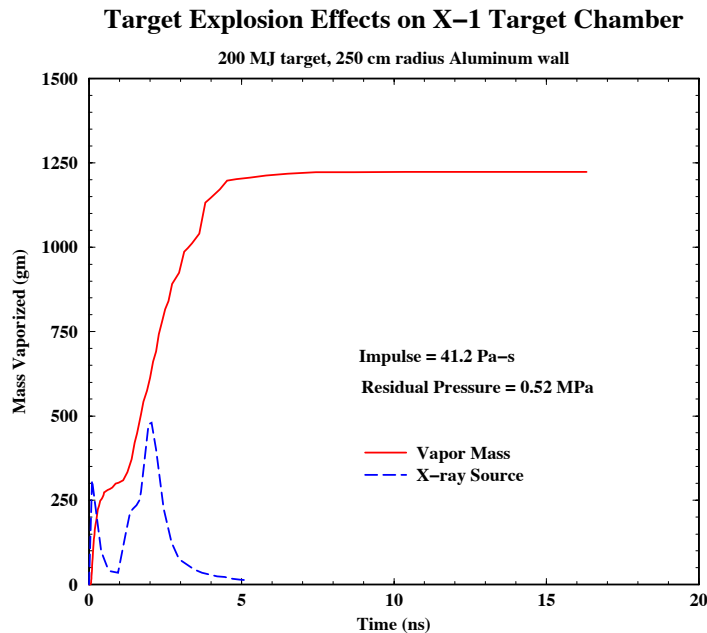


Figure 4.3.1. Mass vaporized from X-1 chamber liner by x-rays from 200 MJ target explosion.

### Target Explosion Effects on X-1 Target Chamber

200 MJ target, 250 cm radius Aluminum wall

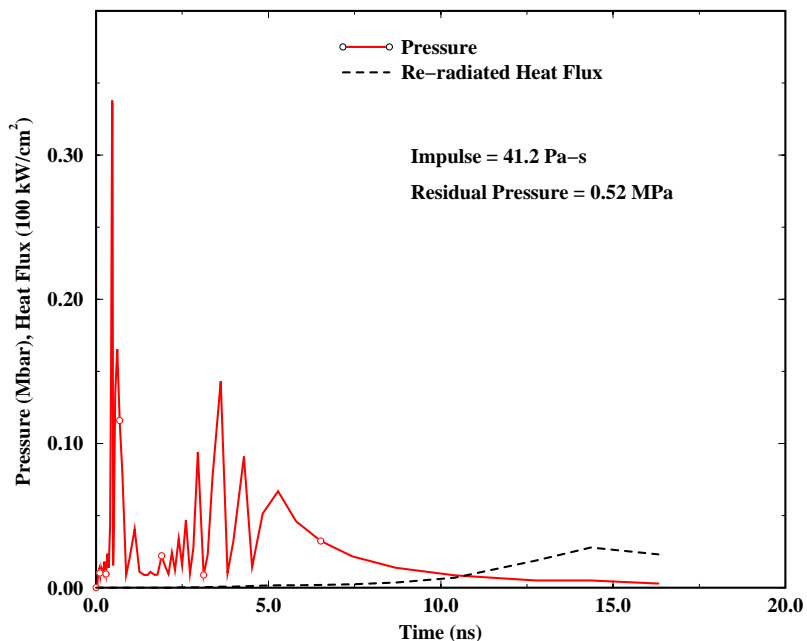


Figure 4.3.2. Pressure and heat flux on inner surface of X-1 chamber liner due to x-rays from 200 MJ target explosion.

### Aluminum X-1 Target Chamber

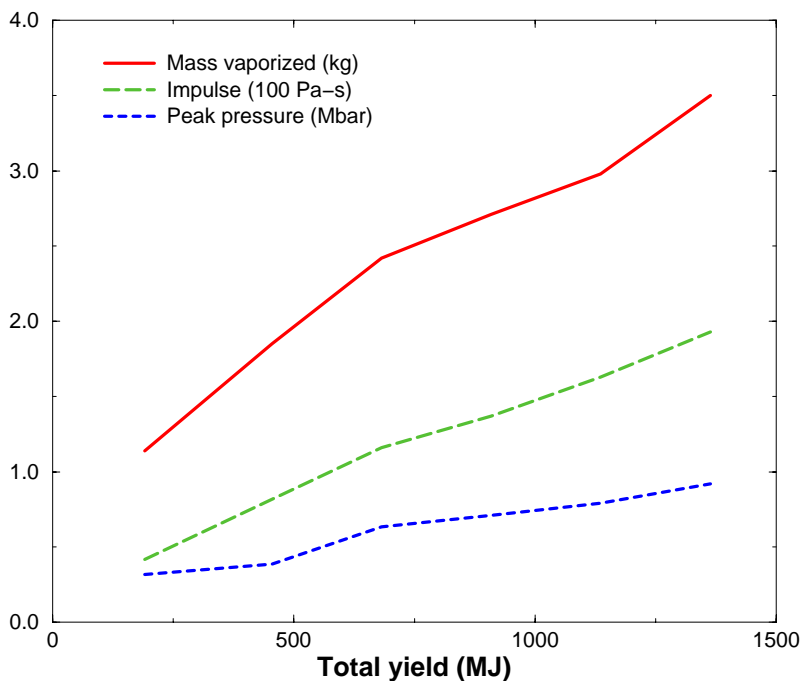


Figure 4.3.3. Mass vaporized, impulse and peak pressure on surface of X-1 chamber liner as a function of target yield.

Table 4.3.1. Response of X-1 Chamber Liner to Target Explosion

Fusion Yield (MJ)	0	200	1000
X-ray Energy (MJ)	16	44	220
X-ray Fluence (J/cm <sup>2</sup> )	20.4	56.0	280
Debris Ion Energy (MJ)	0	12	61
Debris Ion Fluence (J/cm <sup>2</sup> )	0	15	76
Vapor Mass (kg)	0.60	1.22	2.80
Impulse (Pa-s)	18.4	41.2	152
Peak Pressure (MPa)	1.1x10 <sup>5</sup>	3.4x10 <sup>5</sup>	8.9x10 <sup>5</sup>
Residual Pressure (MPa)	0.12	0.52	3.11

Table 4.4.1. Response of X-1 Insulator Stack to Blast Down MITL Gap

Fusion Yield (MJ)	200
Impulse (Pa-s)	154
Peak Pressure (MPa)	0.44
Radiated Fluence (J/cm <sup>2</sup> )	94.5

#### 4.4 MITL and Insulator Stack

The response of the plastic insulator stack to any portion of the target generated blast that propagates down the A-K gap in the MITL's is very important to the water transformer pulsed power option. Such a blast is assumed to be driven by the residual pressure in the mini-chamber, which in some manner finds its way into the MITL. For a 200 MJ target explosion the residual pressure in the mini-chamber is 4.3 MPa and the average carbon vapor density is 58 μg/cm<sup>3</sup>. A BUCKY simulation has been performed in cylindrical geometry for a 300-cm long MITL gap, which is initially at low pressure. The insulator stack is assumed to be at the end of the gap. The results are summarized in Table 4.4.1. A substantial impulse and radiant fluence are applied to the insulator stack by the blast. Density profiles in the gap are shown in Figure 4.4.1, where the details of the rarefaction wave moving down the gap can be seen. Density begins to accumulate against the insulator stack, leading to a long-term pressure loading. This is seen in Figure 4.4.2, where the pressure and heat flux on the insulator stack is plotted against time. From these results, it is clearly possible to prevent this loading with a valve with a 25 μs closing time if it is placed near the stack.

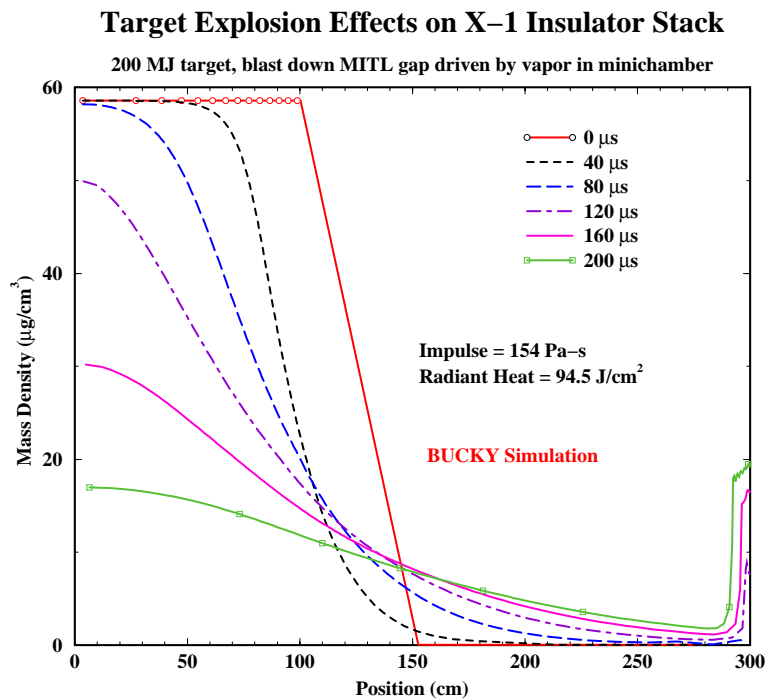


Figure 4.4.1. Density profiles in MITL gap from 200 MJ target explosion.

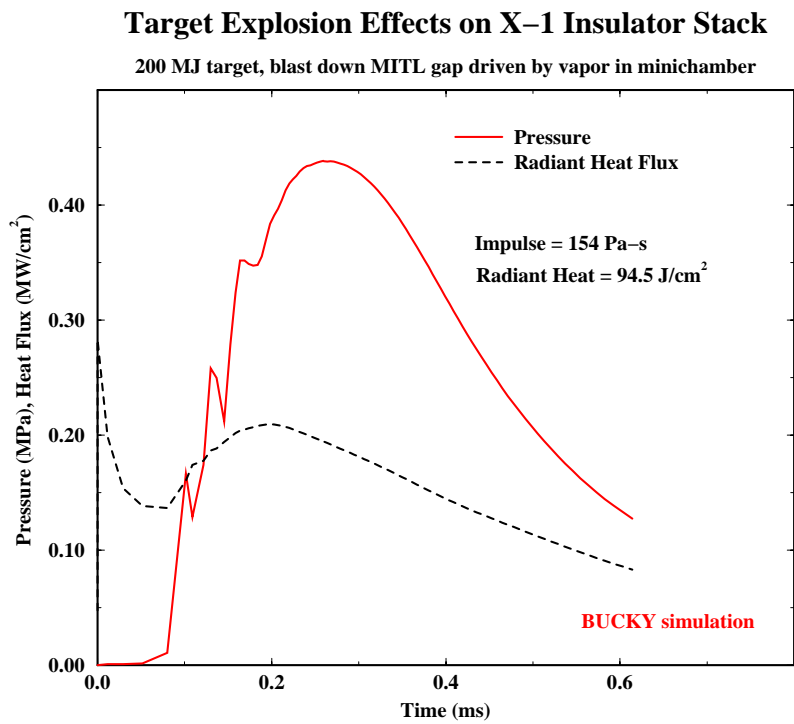


Figure 4.4.2. Pressure and heat flux on inner surface of X-1 insulator stack due to 200 MJ target explosion.

## 4.5 Development Needs

The response of the experiment chamber to x-ray, ion and shrapnel loading is of great importance to the X-1 concept. Additional analysis of the chamber concepts needs to be performed. To have confidence in the X-1 experiment chamber design, the methods of analysis need to be validated by experiments. Additional analysis needs to be performed in the following areas:

- 1-D chamber response for a broad range of likely target, z-pinch and magnetic debris loading. X-ray spectra specific to X-1 targets will become available in the near future and chamber analysis must be calculated using this information. Other target concepts for high energy density experiments will be shot in X-1 that will produce as yet unknown chamber environments. Response to high yield and unusual spectra must be considered. Z-pinch spectra will soon be available for X-1 and the response to these x-rays needs to be considered. This broad survey for responses to various targets should be performed initially in 1-D with the BUCKY code to find the worst conditions.
- Two- and 3-D analysis of chamber response is needed to analyze the flow of vapor and dust into ports and gaps. The vapor and dust is radioactive and confinement schemes need to be analyzed in multiple dimensions.
- Fragmentation and shrapnel needs to be studied. Initial analytic models should be combined with 1-D BUCKY simulations to estimate shrapnel sizes and velocities. Models for fragmentation need to be developed and applied to these BUCKY simulations. Two- and 3-D fragmentation simulations need to be applied to X-1 conditions.
- Flow of vapor and fragments need to be calculated together in multi-phase simulations.
- Melting of the liner needs to be analyzed.
- Magnetic debris needs to be calculated with multi-D fragmentation codes.

Experimental validation needs to be done:

- X-ray vaporization and melting experiments should be performed on Z or Saturn. The models in BUCKY need to be validated. Comparisons with measured impulses, vapor mass, melt mass, and fragment size are needed for BUCKY and fragmentation codes. Experiments need to be performed for all chamber materials (graphite lined Kevlar, aluminum alloy, steel).
- Magnetic debris needs to be measured and compared with fragmentation code predictions.
- Ion debris response needs to be validated with comparisons between RHEPP experiments and BUCKY predictions.

## References for Sections 4 and 4.1

1. MacFarlane, M.E. Sawan, G.A. Moses, P. Wang, and R.E. Olson, "Numerical Simulations of the Explosion Dynamics and Energy Release from high-Gain ICF Targets", University of Wisconsin Fusion Technology Institute Report UWFD-1026 (June 1996).
2. MacFarlane, G.A. Moses, and R.R. Peterson, "BUCKY-1 -- A 1-D Radiation Hydrodynamics Code for Simulating Inertial Confinement Fusion High Energy Density Plasma", University of Wisconsin Fusion Technology Institute Report UWFD-984 (August 1995).
3. "SESAME: The Los Alamos national Laboratory Equation of State Database", LANL Report LA-UR-92-3407, edited by S.P. Lyon and J.D. Johnson (1992).
4. Wang, "ATBASE User's Guide", University of Wisconsin Fusion Technology Institute Report UWFD-984 (December 1993).

## **5. Conclusions**

A preliminary experiment chamber concept has been completed for X-1. This design is compatible with either the long MITL or water transformer pulsed-power concepts. It is also compatible with target diagnostics and remote removal of the chamber. As the pulsed power and experimental requirements evolve the experimental chamber design will require modification.

Preliminary analysis of the chamber has been performed and no issues have arisen for which there is no design solution. Blast effects, radioactivity and mechanical response have been calculated. The general result is that the experimental chamber will need refurbishment after each shot and that after a target explosion with significant fusion yield the operators will not be allowed hands-on access for more than a week. The blast damage is worse at the highest yields. There is clearly an operations price paid for thermonuclear yield, which must be considered when the rate of yield shots is determined.

## **Acknowledgment**

This work is supported by Sandia National Laboratories.